

1 ***A CRISPR/Cas9-BASED APPROACH FOR EDITING IMMORTALISED HUMAN***  
2 ***MYOBLASTS TO MODEL DUCHENNE MUSCULAR DYSTROPHY IN VITRO***

3

4 **P. Soblechero-Martín<sup>1</sup>, E. Albiasu-Arteta<sup>1</sup>, A. Anton-Martinez<sup>1</sup>, I.**  
5 **Garcia-Jimenez<sup>1</sup>, G. González-Iglesias<sup>1</sup>, I. Larrañaga-Aiestaran<sup>1</sup>, A.**  
6 **López-Martinez<sup>1</sup>, J. Poyatos-García<sup>2</sup>, E. Ruiz-Del-Yerro<sup>1</sup>, F. Gonzalez<sup>3</sup>,**  
7 **V. Arechavala-Gomez<sup>1,4</sup>**

8

9 <sup>1</sup>Neuromuscular Disorders, Biocruces Bizkaia Health Research Institute, Barakaldo, Spain

10 <sup>2</sup>La Fe Health Research Institute, Hospital La Fe, Valencia, Spain

11 <sup>3</sup>Pluripotent Stem Cells and Activation of Endogenous Tissue Programs for Organ

12 Regeneration (PR Lab), Institute for Bioengineering of Catalonia (IBEC), Barcelona, Spain

13 <sup>4</sup>Ikerbasque, Basque Foundation for Science, Bilbao, Spain

14

15

16

17

18

19

20 **Address for correspondence:**

21 Prof. Virginia Arechavala-Gomez

22 Biocruces Bizkaia Health Research Institute

23 Barakaldo, Bizkaia, 48903, Spain

24 Phone: +34 946007967

25 E-mail: virginia.arechavalagomez@osakidetza.eus

26 ORCID : 0000-0001-7703-3255

27 **Summary**

28 We report two novel immortalised myoblast culture models for studying Duchenne  
29 muscular dystrophy (DMD), generated through CRISPR/Cas9 gene editing: one  
30 recapitulates a common *DYSTROPHIN (DMD)* deletion and the other a regulatory  
31 mutation leading to *UTROPHIN (UTRN)* ectopic upregulation.

32 **Abstract**

33 CRISPR/Cas9-mediated gene editing may allow treating and studying rare genetic  
34 disorders by respectively, correcting disease mutations in patients, or introducing  
35 them in cell cultures. Both applications are highly dependent on Cas9 and sgRNA  
36 delivery efficiency. While gene editing methods are usually efficiently applied to cell  
37 lines such as HEK293 or hiPSCs, CRISPR/Cas9 editing *in vivo* or in cultured myoblasts  
38 prove to be much less efficient, limiting its use. After a careful optimisation of  
39 different steps of the editing protocol, we established a consistent approach to  
40 generate human immortalised myoblasts disease models through CRISPR/Cas9  
41 editing. Using this protocol we successfully created a coding deletion of exon 52 of  
42 the *DYSTROPHIN (DMD)* gene in wild type immortalised myoblasts modelling  
43 Duchenne muscular dystrophy (DMD), and a microRNA binding sites deletion in the  
44 regulatory region of the *UTROPHIN (UTRN)* gene leading to utrophin upregulation in  
45 in Duchenne muscular dystrophy patient immortalised cultures. Sanger sequencing  
46 confirmed the presence of the corresponding genomic alterations and protein  
47 expression was characterised using myoblots. To show the utility of these cultures  
48 as platforms for assessing the efficiency of DMD treatments, we used them to  
49 evaluate the impact of exon skipping therapy and ezutromid treatment. Our editing  
50 protocol may be useful to others interested in genetically manipulating myoblasts  
51 and the resulting edited cultures for studying DMD disease mechanisms and  
52 assessing therapeutic approaches.

53

54 **KEYWORDS:** Duchenne muscular dystrophy, Dystrophin, Utrophin, Gene edition

55 **INTRODUCTION**

56 **Duchenne muscular dystrophy** (DMD) is a fatal X-linked recessive disease affecting  
57 one out of 3.500-5.000 newborn males. It is commonly caused by deletions disrupting  
58 the open reading frame of the *DYSTROPHIN* (*DMD*) gene causing a lack of dystrophin  
59 protein (Hoffman et al., 1987). Patients carrying out of frame mutations present a  
60 severe phenotype, while those carrying in-frame mutations may result in hypomorphic  
61 alleles, a partially functional dystrophin and milder phenotypes, such as in Becker  
62 muscular dystrophy (BMD)(Anthony et al., 2011). Dystrophin plays a major role in  
63 membrane stabilization during muscle contraction, linking the actin cytoskeleton to  
64 the sarcolemma (Muntoni et al., 2003) and also contributes to extracellular signalling  
65 (Lai et al., 2009). Lack of dystrophin in DMD patients' muscles, leads to progressive  
66 muscle wasting and degeneration. DMD children suffer from loss of ambulation in the  
67 first or second decade of life and premature death by cardiac and respiratory  
68 complications (Eagle et al., 2002).

69 Although no definitive cure for DMD is available, three drugs have been recently  
70 approved by different regulatory agencies. Ataluren, approved by the European  
71 Medicines Agency (EMA), induces readthrough of premature stop codons during  
72 mRNA translation, allowing generating a full length dystrophin protein (Finkel, 2010).  
73 Eteplirsen and golodirsen, approved by the US Food and Drug Administration (FDA),  
74 are antisense oligonucleotides. Eteplirsen targets *DMD* exon 51 and golodirsen, exon  
75 53. Both antisense oligonucleotides modulate splicing by exon skipping, restoring *DMD*  
76 reading frame and leading to a shorter but functional protein (Kinali et al., 2009;  
77 Muntoni et al., 2018). Exon skipping therapies aim to attenuate the phenotype and  
78 phenocopy milder BMD-like genotypes, to potentially improve disease outcome.  
79 Aataluren, eteplirsen and golodirsen are designed for rescuing specific patient  
80 mutations only present respectively in 13%, 13% and 8% of patients (Aartsma-Rus et  
81 al., 2006). It is therefore important to test and assess alternative exon-skipping  
82 strategies targeting other *DMD* exons in different phases of clinical assays (Arechavala-  
83 Gomez et al., 2012). Alternatively, a number of compounds applicable to all DMD  
84 patients are also under evaluation, targeting secondary DMD pathologies or trying to  
85 compensate for the lack of dystrophin.

86 **UTROPHIN** (*UTRN*) is an autosomal paralog of dystrophin, expressed in skeletal muscle  
87 cells during embryonic development, but restricted to neuromuscular and  
88 myotendinous junctions in the mature muscle fibre (Tinsley et al., 1992).  
89 Overexpression of utrophin in skeletal muscle in DMD animal models can partially  
90 compensate the lack of dystrophin and improve DMD phenotype (Cerletti et al., 2003;  
91 Tinsley et al., 1998; Tinsley et al., 1996). Importantly, ectopic and high levels of  
92 utrophin in myoblasts are not associated with toxicity, making utrophin upregulation  
93 an interesting therapeutic strategy applicable to all patients, no matter their particular  
94 mutation (Fairclough et al., 2013; Fisher et al., 2001). Ezutromid/SMT-C1100 was the  
95 first utrophin modulator evaluated in clinical assays, but was recently abandoned due  
96 to lack of evidence of utrophin restoration, nor clinical improvement for patients  
97 (Ricotti et al., 2016; Tinsley et al., 2015). Alternatively, other studies proposed new  
98 strategies to upregulate *UTRN* by removing the binding sites of microRNAs repressing  
99 *UTRN* expression through gene editing (Amenta et al., 2011; Goyenvalle et al., 2010;  
100 Morgoulis et al., 2019; Pisani et al., 2018).

101 **CRISPR/Cas9** currently represents the most efficient and versatile genome-engineering  
102 tool, allowing introducing small and large DNA modifications, including large genomic  
103 deletions in different cell types and organisms (Wright et al., 2016). Hence, in the  
104 presence of two single guide (sg) RNAs targeting two different loci on the same  
105 chromosome, Cas9 can induce two DNA double strand breaks (DSBs), leading in some  
106 cases to deletion of the excised DNA segment through repair by the non-homologous  
107 end joining (NHEJ) pathway (He et al., 2015). Similar to antisense oligo-mediated exon  
108 skipping therapies at RNA level, CRISPR/Cas9 can therefore be used to remove  
109 mutations by deleting mutated exons and restore the open reading frame of the *DMD*  
110 gene (Amoasii et al., 2018; Ousterout et al., 2015; Young et al., 2016). The advantage  
111 of this approach is that the genetic modification, once introduced, is stable over cell  
112 cycles. However, its efficiency is currently too low to provide a real therapeutic  
113 alternative *in vivo*, not even mentioning immunogenicity and off-target problems  
114 linked with the use of Cas9 (Charlesworth et al., 2019).

115 In order to easily and rapidly assess the efficiency of current and novel therapies to  
116 treat DMD, *in vitro* cellular models are particularly useful. However, only a few human

117 immortalized muscle cell lines derived from DMD patients are currently available  
118 (Mamchaoui et al., 2011). Due to the wide spectrum of DMD mutations and the  
119 difficulties to obtain DMD patient muscle biopsies, an efficient approach to edit DMD  
120 mutations in immortalised myoblasts would be extremely valuable to generate a more  
121 exhaustive panel of DMD-myoblast models. Such lines would provide a powerful  
122 resource for *in vitro* drug screening and study disease rescue mechanisms.

123 Here, we report an optimised CRISPR/Cas9 approach to edit myoblasts to create DMD  
124 disease models. We successfully used this protocol to created two new cell lines: in  
125 objective 1, control myoblasts were edited to remove *DMD* exon 52 (a common  
126 mutation in DMD patients); in objective 2, DMD patient's myoblasts were edited to  
127 generate a utrophin ectopic expression rescue model by deleting miRNA binding sites  
128 in *UTRN* regulatory region.

## 129 **RESULTS**

### 130 **Optimisation of gene edition in myoblasts and generation of two new cell culture** 131 **models.**

- 132 • Guide selection for CRISPR/Cas9 system.

133 We had two different gene editing objectives: **objective 1** aimed to delete exon 52 of  
134 the *DMD* gene to generate a disease model in control immortalised myoblasts;  
135 **objective 2** was to delete in the *UTRN* gene a binding site for *UTRN*-repressing  
136 microRNAs in DMD immortalized human myoblasts.

137 Our strategy to perform CRISPR/Cas9 editing in myoblasts was to design two sgRNAs  
138 flanking the region to be deleted in order to generate two DSBs leading to removal of  
139 that region (Figure 1).

- 140 • Testing sgRNAs in HEK293 cultures.

141 As transfection of myoblast is very inefficient, all the different combinations of the  
142 sgRNAs cutting before and after the target region (5x5), were tested in HEK293  
143 cultures first (Figure 2). The combination of sgRNAs that was most efficient in HEK293  
144 cells for each objective was selected to be used in the transfection of human  
145 immortalized myoblasts.

146

147 • Myoblast transfection and single cell sorting workflow

148 Myoblasts were transfected with the two GFP-plasmids encoding each of the selected  
149 sgRNA selected for the edition of the target region. After comparing four different  
150 transfection reagents and an electroporation method, transfection of myoblasts with  
151 Viafect® (Promega, Spain) was selected (See Supplementary figure 3). After  
152 transfection, GFP-positive cells were sorted by FACS (See Supplementary figure 3),  
153 seeded as single cells in 96 well plates (five plates per condition) and expanded in  
154 culture (see schematic workflow in Figure 3).

155 • Selection of edited clones:

156 A limited number of clones derived from GFP-positive single cells grew enough for  
157 further analysis: 20/314 for objective 1 and 35/480 for objective 2. To confirm the  
158 presence of the desired deletions, a genomic PCR was performed with specific primers  
159 for each targeted gene (Figure 4 and Supplementary Table 1). Amplicons  
160 corresponding in size with the expected deletions were analysed by Sanger sequencing  
161 and the expected deletions were confirmed in all the positive clones, which  
162 corresponds to edition efficiency between 5-6%. To evaluate any potential off-target  
163 effects, each selected sgRNA was analysed *in silico* using the bioinformatics web-tool  
164 CRISPOR (Haeussler et al., 2016) . We selected the six more likely off-target sites for  
165 each sgRNA and analysed each one of them through PCR, followed by Sanger  
166 sequencing in edited clones (Table 1). We found no off-target effects in any of the 12  
167 sites studied for each clone sites (Supplementary figure 1).

168 **Analysis of dystrophin and utrophin expression in edited clones.**

169 We compared dystrophin expression in myotubes of the DMD  $\Delta$ 52-Model to controls  
170 and DMD cultures, and confirmed that it was abolished by immunohistochemistry  
171 (Figure 5A), western blot analysis (Figure 5B) and myoblots (Figure 5C). Dystrophin  
172 levels in this model, where exon 52 had been removed by CRISPR/Cas9 edition, were  
173 statistically no different than those seen in a culture from a DMD patient.

174

175 It was difficult to corroborate by immunocytochemistry the increase of utrophin  
176 expression between unedited DMD and DMD-UTRN-Model myotubes (Figure 5D) but

177 this increase was evident by western blot (a 175% increase, Figure 5E) and myoblot  
178 analysis (close to 50% increase, Figure 5F).

179 We also evaluated myoblast differentiation in all the cultures by myoblot, and we  
180 could observe a decrease in the MF20 differentiation marker in all the edited clones,  
181 no matter the deletion, compared with their corresponding controls (Supplementary  
182 Figure 2).

183

#### 184 **Evaluation of therapies in newly generated model cell lines.**

185 To assess if the DMD $\Delta$ 52-Model cell culture could be useful to test potential mutation  
186 specific therapies for DMD, we evaluated the exon skipping efficiency of an antisense  
187 oligonucleotide in this culture. We treated the DMD $\Delta$ 52-Model cultures with an  
188 antisense oligonucleotide drug that can skip exon 51 (van Deutekom et al., 2007) and  
189 restore *DMD* open reading frame. After treatment with this drug, we confirmed that  
190 exon skipping had taken place at RNA level (Figure 6A), and the restoration of  
191 dystrophin expression by myoblot analysis (Figure 6B).

192

193 To test our DMD-UTRN-Model as a positive utrophin overexpression control, we  
194 cultured it alongside the original unedited DMD cultures, which we treated with  
195 several concentrations of ezutromid and we evaluated the expression of utrophin in all  
196 cultures. We observed that utrophin was hardly modified in DMD cultures treated with  
197 ezutromid while a robust overexpression was confirmed in the DMD-UTRN-Model  
198 compared to the unedited DMD cultures. (Figure 6C)

199

#### 200 **DISCUSSION**

201 CRISPR/Cas9 as a possible therapeutic approach for DMD has been explored in the  
202 past in *in vitro* models of the disease. In most of these cases, a “permanent” exon  
203 skipping approach was selected where a shorter protein would be produced  
204 (Ousterout et al., 2015; Young et al., 2016), while in some others full length dystrophin  
205 was the result of the edition (Lattanzi et al., 2017; Li et al., 2014; Wojtal et al., 2015).  
206 After several studies showed efficacy also in mice models (Long et al., 2016; Nelson et  
207 al., 2016; Tabebordbar et al., 2016), a recent study in dogs is currently the most

208 advanced example of its application to DMD (Amoasii et al., 2018). Before this can be a  
209 credible therapeutic option, several delivery and manufacturing problems will need to  
210 be overcome. In the meantime, this methodology is very useful for researchers looking  
211 for disease models: muscle biopsies are not routinely collected during diagnosis of this  
212 disorder and seldom cultured. This means there are few good culture models of the  
213 disease. Another tool created to facilitate research, was the immortalisation of some  
214 of the available cultures (Mamchaoui et al., 2011), which increases the possibility of  
215 performing more experiments with a given culture. We have used immortalised  
216 cultures to further increase this possibility.

217 Our preliminary experiments to perform gene edition in the *DMD* gene of HEK293 cells  
218 were successful. However, a big roadblock was encountered in the form of very poor  
219 transfection efficiency of our chosen gene editing reagents in myoblasts (Ousterout et  
220 al., 2015; Wojtal et al., 2015). This is a problem shared by many research laboratories,  
221 and we consider that our protocol, although still not very efficient, may help those  
222 facing the same difficulties. We have successfully applied this protocol to edit 2  
223 different regions in two different cell backgrounds (Control and DMD), and we  
224 consider that those described and fully characterised in this manuscript could be  
225 relevant research models that we would be happy to share. The first of these models is  
226 an immortalised DMD disease cell culture model, (DMD $\Delta$ 52-Model) that lacks exon 52  
227 of the *DMD* gene, which disrupts the ORF and dystrophin expression. This model could  
228 be useful to evaluate mutation-independent drug treatments, and also exon skipping  
229 drugs that aim to skip exons 51 or 53 (Arechavala-Gomez et al., 2007; Popplewell et  
230 al., 2010) as skipping either exon in this case would restore the ORF and dystrophin  
231 expression. We have demonstrated that DMD $\Delta$ 52-Model lacks dystrophin expression  
232 and that this can be reverted through treatment with an exon 51 skipping drug.

233 An immortalised cell culture model constitutively expressing utrophin, DMD-UTRN-  
234 Model, is both a proof of principle of a possible therapeutic option to overexpress  
235 utrophin as a substitute for dystrophin, and a valuable research tool. The search of  
236 drugs that could overexpress utrophin is ongoing (Guiraud and Davies, 2017) after the  
237 recent failure of ezutromid to show relevant results in clinical trials. Many research  
238 projects, including drug re-purposing screening, are ongoing to find new candidates to



239 test in clinical trials. However, there are no reliable positive controls that could be used  
240 to compare such treatments. We propose that our cell model could serve that  
241 purpose, offering researchers useful custom controls for their studies. We have tested  
242 this hypothesis and compared the stable utrophin overexpression quantified in the  
243 DMD-UTRN-Model with the one that is obtained after treatment with ezutromid, the  
244 lead market candidate in this field until very recently, with positive results. Previous  
245 studies in muscle sections show that DMD patients already overexpress utrophin, in  
246 many cases 4 to 5-fold the levels seen in control muscle sections (Arechavala-Gomez  
247 et al., 2010). Our choice to target this particular *UTR* region, increases basal  
248 overexpression in DMD cultures, and the amount of overexpression varies significantly  
249 when evaluated by western blot (more than 2.5 times) or our preferred method,  
250 myoblots (close to 1.5 times). We like to consider that myoblot evaluation reflects  
251 more closely the actual protein expression, as it is not subjected to many of the  
252 inherent problems of western blotting when evaluating very large proteins (Ruiz-Del-  
253 Yerro et al., 2018). This is why we cannot comment yet on the differences in  
254 expression between our study and other published studies that also aimed to  
255 overexpress utrophin by gene edition, but which 1) targeted different promoters  
256 regions (*UTRN A* or *UTRN B*) of utrophin and 2) evaluated their results by western blot  
257 analysis (Wojtal et al., 2015). We would be interested on studying this matter further  
258 to analyse the differences in utrophin expression when targeting different regions.

259 As a conclusion, we have optimised a gene edition method to be applied to myoblasts,  
260 a rather difficult target, and expect our experience to be useful to other muscle  
261 researchers. The two new cell culture models described are already being used as  
262 efficient tools in our search for new therapies for DMD and we are looking forward  
263 expanding those experiments.

264

## 265 **MATERIALS AND METHODS**

### 266 **CRISPR/Cas9 tools**

267 Each edition requires 2 sgRNAs. Specific sgRNA guides were designed using the online  
268 bioinformatics tool <http://crispr.mit.edu> (Ran et al., 2013). Ten different guides (five  
269 before and five after the target region) were designed targeting exon 52 flanking  
270 regions in *DMD* gene and another ten targeting a repressor binding site in the UTR 3'  
271 region of *UTRN* gene and selected according to their score number (Figure 1). They  
272 were cloned into a plasmid containing *Cas9* from *S. pyogenes* with 2A-EGFP  
273 pSpCas9(BB)-2A-GFP (PX458) (Addgene plasmid # 48138, deposited by Feng Zhang. All  
274 sgRNAs were cloned using BbsI sites.

### 275 **Cell cultures**

276 Immortalized myoblasts derived from muscle biopsies from healthy controls and DMD  
277 patients were provided by the CNMD Biobank, London, UK and the Institut de  
278 Myologie Paris, France, and cultured using skeletal muscle medium (SMM) (Promocell,  
279 Germany) and differentiation media as previously described (Ruiz-Del-Yerro et al.,  
280 2018).

281 Human embryonic kidney 293 (HEK 293) cells, used in the preliminary selection of the  
282 best sgRNA combinations for our experiments, were purchased from the European  
283 Collection of Authenticated Cell cultures (ECCAC) via Sigma-Aldrich, Spain, and  
284 maintained following the manufacturer's protocols.

### 285 **Cell culture transfection**

286 All different sgRNAs combinations were transfected into HEK 293 cells using  
287 lipofectamine 2000® (Thermo Fisher Scientific), according to the manufacturer's  
288 protocol. Myoblasts seeded in 6 well plates at 70-80% confluence were transfected  
289 with 1.5ug of each plasmid with the most efficient guide RNA combination using  
290 ViaFect™ (Promega) tranfection reagent (1:5 ratio).

291

### 292 **FACS Sorting of GFP positive myoblasts:**

293 48 hours after transfection myoblasts were trypsinized and collected for FACS sorting  
294 (fluorescence activated cell sorting), at the Cell Analytics Facility (BD FACS Jazz)

295 Achucarro Basque Center for Neuroscience - (Leioa, Spain). GFP-positive cells were  
296 seeded individually in 96 well plates for clonal selection. The first colonies were visible  
297 around 7 days post-sorting. Clones were expanded from single cell to near-confluence  
298 and expanded into larger well plates to be harvested 15-30 days post-sorting.  
299 Myoblasts often developed elongated and stressed shapes during this clonal expansion  
300 after single cell sorting. Harvested cultures were aliquoted: some aliquots were frozen  
301 for archival; others were pelleted for DNA analysis, while replicates were cultured  
302 further for characterization by immunocytochemistry, western blot and myoblots.

303

#### 304 **Analysis of gene edition**

305 DNA was extracted from cell pellets using a QIAamp® DNA Mini Kit, Qiagen. PCR  
306 amplification targeting the edited regions was carried out using Taq DNA Polymerase  
307 (Recombinant), Invitrogen, under the following conditions: preheating 3' 94°C, 25  
308 cycles of 94° for 3', 94° 20'', 63° 20'', 72° 1' and 72° 5' and DMD-Seq-D52-DOWN-F2  
309 and DMD-Seq-D52-DOWN-R2 primers (see Table 1). PCR products were resolved in 2%  
310 TAE-agarose gels and purified with QIAquick® Gel extraction Kit, Qiagen. PCR  
311 amplicons corresponding to the expected length were analysed by Sanger sequencing  
312 at the sequencing platform of Biocruces Bizkaia Health Research Institute using DMD-  
313 Seq-D52-DOWN-F2 and DMD-Seq-D52-DOWN-R2 primers (see Table 1).

#### 314 **Off-target analysis of mutations in clonal lines**

315 Potential off-target region loci of each sgRNA used were predicted using CRISPOR  
316 bioinformatics tool <http://crispor.tefor.net/>. The six most probable off-target  
317 sequences per guide were analysed in the edited clones using genomic PCR and Sanger  
318 sequencing. Primer sets flanking off-target sites and the corresponding internal  
319 primers used for Sanger sequencing are listed in table 2.

#### 320 **Primary Antibodies**

321 Anti-dystrophin: Dys1 (Leica Biosystems), Mandys1, Mandys106 (The MDA Monoclonal  
322 Antibody Resource)

323 Anti-utrophin: Mancho7 (The MDA Monoclonal Antibody Resource)

324

325

### 326 **Immunostaining assays**

327 Original and edited clones for objectives 1 (DMD $\Delta$ 52-Model) and 2 (DMD-UTRN-  
328 Model) were cultured and immunostained for dystrophin or utrophin expression.  
329 Edited clones were seeded into chamberslides and treated with a MyoD virus, (Applied  
330 Biological Materials Inc, Canada) to facilitate differentiation into myotubes (Roest et  
331 al., 1996). After seven days differentiating, samples were fixed with 4% PFA. Cultures  
332 were permeabilised with Triton 0.5% and then blocked for half an hour with BSA 2%.  
333 Afterwards, immunostaining was performed overnight at 4°C with the required  
334 antibodies. Primary antibodies used for dystrophin staining were a mix of Dys1,  
335 Mandys1 and Mandys106 at 1:100 dilution and for utrophin staining was Mancho 7  
336 diluted at 1:50. The following day, after being washed with PBS Tween 0.1%, cells were  
337 stained with Alexa Fluor 488 goat anti-mouse (Invitrogen) for 1 hour at room  
338 temperature. Hoechst 1/2000 was used for nuclei staining and chamberslides were  
339 mounted with PermaFluor™ Aqueous Mounting Medium (Thermoscientific). Images  
340 were captured with a LEICA DMI 6000B microscope at the Microscopy Platform at  
341 Biocruces Bizkaia Health Research Institute.

### 342 **In-cell western assay (myoblots)**

343 Myoblots were performed as described before (Ruiz-Del-Yerro et al., 2018). In short,  
344 clones were seeded in 96-well plates and incubated for 24 h in SMMC, after which they  
345 were treated with MyoD virus and incubated in differentiation media for 7 days. Then,  
346 plates were fixed with ice-cold methanol, permeabilised and blocked before incubation  
347 with the required primary antibodies overnight: anti-dystrophin mix (Dys1, Mandys1  
348 and Mandys106 at 1:100), anti-utrophin (Mancho 7 antibody at 1:50), and anti-myosin  
349 heavy chain antibody (MF20 at 1:100) that was used to evaluate differentiation. Next  
350 day, plates were incubated with the secondary antibodies. Biotin-mediated  
351 amplification (Abcam 6788 goat antimouse IgG biotin 1:2000) was used to increase  
352 dystrophin signal. Secondary antibodies, IRDye 800cw streptavidin 1:2000 and IRDye  
353 800CW goat anti-mouse 1:500, were prepared together with CellTag 700 Stain (LI-  
354 COR® Biosciences) at 1:1000 dilution and incubated for 1 hour at RT and protected  
355 from light. After incubation, plates were analysed using the Odyssey® CLx Imager (LI-  
356 COR® Biosciences).

### 357 **Treatment with antisense exon skipping drugs**

358 Cultures in 96 wells and P6 wells were treated with a 2'MOE-phosphorotioate  
359 antisense oligonucleotide (AO) aiming to skip *DMD* exon 51 (5'-[  
360 T\*C\*A\*A\*G\*G\*A\*A\*G\*A\*T\*G\*G\*C\*A\*T\*T\*T\*C\*T]-3', Eurogentec, Belgium) by  
361 transfection with Lipofectamine as described in (Arechavala-Gomez et al., 2007;  
362 Popplewell et al., 2010) and analysed by either myoblot (96 well plates) or RT-PCR  
363 (pellets extracted from 6 well plates).

### 364 **RT-PCR**

365 RNA was extracted from cell pellets (RNeasy mini kit, Qiagen) according to the  
366 manufacturer's protocol. Reverse transcription of the samples was performed using  
367 (SuperScrip™ IV Reverse Transcriptase, Invitrogen) according to the manufacturer's  
368 protocol. cDNA samples were amplified by nested PCR using specific primers sets  
369 (supplementary table 1) and Taq DNA Polymerase (Recombinant), Invitrogen, as  
370 described in (Arechavala-Gomez et al., 2007). Samples were resolved in TAE-agarose  
371 and PCR amplicons of interest were first analysed with Gel Doc™ EZ Imager, BIORAD  
372 and then purified with (QIAquick® Gel extraction Kit, QIAGEN) for sequencing analysis.  
373 Before DNA extractions bands were semiquantify using Image J.

### 374 **Treatment with utrophin overexpression drugs**

375 Ezutromid was diluted first in DMSO and finally in differentiation medium to different  
376 concentrations and added to myoblasts in 96 well plates 7 days after differentiation.  
377 Twenty four hours after treatment, medium was removed and plates were fixed with  
378 ice-cold methanol for myoblot analysis.

379

### 380 **Western blot**

381 Cell cultures were seeded into P6 plates and trypsinized after 7 days of differentiation.  
382 Then, cell pellets were solubilized in lysis/loading buffer and denatured at 95°C for 5  
383 min. The samples were loaded onto a NuPAGE® Novex® 3–8% Tris-Acetate Gel3–8%  
384 (Thermo Fisher Scientific) and run in Novex Tris-Acetate SDS Running Buffer (Thermo  
385 Fisher Scientific) for 60 min at 70 V + 120 min at 150 V at 4°C. Protein wet transfer was  
386 performed overnight at 4°C using an Immobilon®-FL PVDF membrane (Merck™). Next  
387 day, membranes were stained with Revert™ 700 Total Protein Stain (Li-Cor) for total

388 protein measurement, blocked with Intercept (PBS) Blocking Buffer (Li-Cor) for 2 hours  
389 and incubated overnight at 4°C with the primary antibodies (1/200 anti-dystrophin  
390 antibody Abcam15277, 1/50 anti-utrophin antibody Mancho 7 or 1/500 anti  $\alpha$ -actinin  
391 antibody, Sigma-Aldrich A7732). After washing steps with PBS-Tween 0.1%,  
392 membranes were incubated with secondary antibodies for 1 hour (1/5000 IRDye  
393 800CW goat anti-rabbit 926–32211 or IRDye 680RD goat anti-mouse 926-68070, Li-  
394 Cor) at room temperature, washed again and scanned using an Odyssey Clx imaging  
395 system. Bands quantification was performed using Image Studio™ software.

396

### 397 **ACKNOWLEDGEMENTS**

398 We acknowledge the use of cell cultures provided by the Queen Square Centre for  
399 Neuromuscular Disorders BioBank (CNMD Biobank, London, UK) and the Institut de  
400 Myologie (Paris, France, immortalised cultures).

401 We gratefully acknowledge the use of the antibodies provided by Professor Glenn  
402 Morris from the Muscular Dystrophy Association (MDA) Monoclonal Antibody  
403 Resource, which distributes free antibodies for research in neuromuscular diseases  
404 worldwide from Oswestry, United Kingdom.

405 The MF20 antibody developed by D.A. Fischman, Weill Cornell Medical College, was  
406 obtained from the Developmental Studies Hybridoma Bank, created by the NICHD of  
407 the NIH and maintained at The University of Iowa, Department of Biology, Iowa City, IA  
408 52242.

409 Cell sorting experiments were performed at the Cell Analytics Facility at Achucarro-  
410 Basque Centre of Neuroscience (Leioa, Spain).

411 We would like to thank Ms. Karmele Alapont-Celaya for her assistance in the  
412 completion of some laboratory tasks during this project. Drs. Gustavo Pérez-Nanclares  
413 and Ana Belén de la Hoz at the Genetics-Genomics Facility, Biocruces Bizkaia Health  
414 Research Institute, are also gratefully acknowledged for their help with sequencing  
415 reactions. Special thanks are due to Drs. Maria Dolores-García Vázquez at the Cell

416 Culture Facility and Dr Javier Díez-García at the Microscopy Facility, both at Biocruces  
417 Bizkaia Health Research Institute, for their assistance at their corresponding platforms.

#### 418 **COMPETING INTERESTS**

#### 419 **FUNDING**

420 This work was supported by funding from Health Institute Carlos III (ISCIII, Spain) and  
421 the European Regional Development Fund, (ERDF/FEDER), ‘A way of making Europe’:  
422 Grant PI15/00333; Basque Government (grants 2016111029 and 2016111091) and  
423 Duchenne Parent Project Spain (grant 05/2016). P. S-M holds a Rio Hortega Fellowship  
424 from ISCIII (CM19/00104). V.A-G holds a Miguel Servet Fellowship from the ISCIII  
425 (CP117/00004), part-funded by ERDF/FEDER. V.A-G also acknowledges funding from  
426 Ikerbasque (Basque Foundation for Science). F. G is supported by a Ramon y Cajal  
427 Grant in Biomedicine (RYC-2014-16751) from the Ministry of Economy and  
428 Competitiveness (MINECO), Spain.

#### 429 **DATA AVAILABILITY**

430 Under request

#### 431 **AUTHOR CONTRIBUTIONS STATEMENT**

432 P S-M, formal analysis, investigation, data curation, writing or original draft, review and  
433 editing, visualization, supervision.

434 E. A-A, investigation, data curation, writing -review and editing.

435 A. A-M, investigation, writing - review and editing.

436 I. G-J, methodology, investigation, review and editing, supervision.

437 G. G-I, investigation, writing - review and editing.

438 I. L-A, investigation, writing - review and editing.

439 A. L-M, investigation, writing - review and editing. J. P-G, investigation, writing -  
440 review and editing.

441 E. R-D-Y, methodology, investigation, writing-review and editing, supervision.

442 F. G conceptualization, formal analysis, writing-review and editing.

443 V. A-G: conceptualization, methodology, formal analysis, investigation, resources, data  
444 curation, writing or original draft, review and editing, visualization, supervision, project  
445 administration and funding acquisition.

446 **REFERENCES**

- 447 **Aartsma-Rus, A., Van Deutekom, J. C., Fokkema, I. F., Van Ommen, G. J. and Den**  
448 **Dunnen, J. T.** (2006). Entries in the Leiden Duchenne muscular dystrophy mutation database:  
449 an overview of mutation types and paradoxical cases that confirm the reading-frame rule.  
450 *Muscle Nerve* **34**, 135-44.
- 451 **Amenta, A. R., Yilmaz, A., Bogdanovich, S., McKechnie, B. A., Abedi, M., Khurana, T.**  
452 **S. and Fallon, J. R.** (2011). Biglycan recruits utrophin to the sarcolemma and counters  
453 dystrophic pathology in mdx mice. *Proc Natl Acad Sci U S A* **108**, 762-7.
- 454 **Amoasii, L., Hildyard, J. C. W., Li, H., Sanchez-Ortiz, E., Mireault, A., Caballero, D.,**  
455 **Harron, R., Stathopoulou, T. R., Massey, C., Shelton, J. M. et al.** (2018). Gene editing restores  
456 dystrophin expression in a canine model of Duchenne muscular dystrophy. *Science*.
- 457 **Anthony, K., Cirak, S., Torelli, S., Tasca, G., Feng, L., Arechavala-Gomez, V., Armaroli,**  
458 **A., Guglieri, M., Straathof, C. S., Verschuuren, J. J. et al.** (2011). Dystrophin quantification and  
459 clinical correlations in Becker muscular dystrophy: implications for clinical trials. *Brain* **134**,  
460 3547-59.
- 461 **Arechavala-Gomez, V., Anthony, K., Morgan, J. and Muntoni, F.** (2012). Antisense  
462 oligonucleotide-mediated exon skipping for Duchenne muscular dystrophy: progress and  
463 challenges. *Curr Gene Ther* **12**, 152-60.
- 464 **Arechavala-Gomez, V., Graham, I. R., Popplewell, L. J., Adams, A. M., Aartsma-Rus,**  
465 **A., Kinali, M., Morgan, J. E., van Deutekom, J. C., Wilton, S. D., Dickson, G. et al.** (2007).  
466 Comparative analysis of antisense oligonucleotide sequences for targeted skipping of exon 51  
467 during dystrophin pre-mRNA splicing in human muscle. *Hum Gene Ther* **18**, 798-810.
- 468 **Arechavala-Gomez, V., Kinali, M., Feng, L., Brown, S. C., Sewry, C., Morgan, J. E. and**  
469 **Muntoni, F.** (2010). Immunohistological intensity measurements as a tool to assess  
470 sarcolemma-associated protein expression. *Neuropathol Appl Neurobiol* **36**, 265-74.
- 471 **Cerletti, M., Negri, T., Cozzi, F., Colpo, R., Andreetta, F., Croci, D., Davies, K. E.,**  
472 **Cornelio, F., Pozza, O., Karpati, G. et al.** (2003). Dystrophic phenotype of canine X-linked  
473 muscular dystrophy is mitigated by adenovirus-mediated utrophin gene transfer. *Gene Ther*  
474 **10**, 750-7.
- 475 **Charlesworth, C. T., Deshpande, P. S., Dever, D. P., Camarena, J., Lemgart, V. T.,**  
476 **Cromer, M. K., Vakulskas, C. A., Collingwood, M. A., Zhang, L., Bode, N. M. et al.** (2019).  
477 Identification of preexisting adaptive immunity to Cas9 proteins in humans. *Nat Med* **25**, 249-  
478 254.
- 479 **Eagle, M., Baudouin, S. V., Chandler, C., Giddings, D. R., Bullock, R. and Bushby, K.**  
480 (2002). Survival in Duchenne muscular dystrophy: improvements in life expectancy since 1967  
481 and the impact of home nocturnal ventilation. *Neuromuscul Disord* **12**, 926-9.
- 482 **Fairclough, R. J., Wood, M. J. and Davies, K. E.** (2013). Therapy for Duchenne muscular  
483 dystrophy: renewed optimism from genetic approaches. *Nat Rev Genet* **14**, 373-8.
- 484 **Finkel, R. S.** (2010). Read-through strategies for suppression of nonsense mutations in  
485 Duchenne/ Becker muscular dystrophy: aminoglycosides and ataluren (PTC124). *J Child Neurol*  
486 **25**, 1158-64.
- 487 **Fisher, R., Tinsley, J. M., Phelps, S. R., Squire, S. E., Townsend, E. R., Martin, J. E. and**  
488 **Davies, K. E.** (2001). Non-toxic ubiquitous over-expression of utrophin in the mdx mouse.  
489 *Neuromuscul Disord* **11**, 713-21.
- 490 **Goyenvalle, A., Babbs, A., Powell, D., Kole, R., Fletcher, S., Wilton, S. D. and Davies,**  
491 **K. E.** (2010). Prevention of dystrophic pathology in severely affected dystrophin/utrophin-  
492 deficient mice by morpholino-oligomer-mediated exon-skipping. *Mol Ther* **18**, 198-205.
- 493 **Guiraud, S. and Davies, K. E.** (2017). Pharmacological advances for treatment in  
494 Duchenne muscular dystrophy. *Curr Opin Pharmacol* **34**, 36-48.
- 495 **Haeussler, M., Schönig, K., Eckert, H., Eschstruth, A., Mianné, J., Renaud, J.-B.,**  
496 **Schneider-Maunoury, S., Shkumatava, A., Teboul, L., Kent, J. et al.** (2016). Evaluation of off-



- 497 target and on-target scoring algorithms and integration into the guide RNA selection tool  
498 CRISPOR. *Genome Biology* **17**, 148-148.
- 499 **He, Z., Proudfoot, C., Mileham, A. J., McLaren, D. G., Whitelaw, C. B. and Lillico, S. G.**  
500 (2015). Highly efficient targeted chromosome deletions using CRISPR/Cas9. *Biotechnol Bioeng*  
501 **112**, 1060-4.
- 502 **Hoffman, E. P., Brown, R. H., Jr. and Kunkel, L. M.** (1987). Dystrophin: the protein  
503 product of the Duchenne muscular dystrophy locus. *Cell* **51**, 919-28.
- 504 **Kinali, M., Arechavala-Gomez, V., Feng, L., Cirak, S., Hunt, D., Adkin, C., Guglieri, M.,**  
505 **Ashton, E., Abbs, S., Nihoyannopoulos, P. et al.** (2009). Local restoration of dystrophin  
506 expression with the morpholino oligomer AVI-4658 in Duchenne muscular dystrophy: a single-  
507 blind, placebo-controlled, dose-escalation, proof-of-concept study. *Lancet Neurol* **8**, 918-28.
- 508 **Lai, Y., Thomas, G. D., Yue, Y., Yang, H. T., Li, D., Long, C., Judge, L., Bostick, B.,**  
509 **Chamberlain, J. S., Terjung, R. L. et al.** (2009). Dystrophins carrying spectrin-like repeats 16  
510 and 17 anchor nNOS to the sarcolemma and enhance exercise performance in a mouse model  
511 of muscular dystrophy. *J Clin Invest* **119**, 624-35.
- 512 **Lattanzi, A., Duguez, S., Moiani, A., Izmiryan, A., Barbon, E., Martin, S., Mamchaoui,**  
513 **K., Mouly, V., Bernardi, F., Mavilio, F. et al.** (2017). Correction of the Exon 2 Duplication in  
514 DMD Myoblasts by a Single CRISPR/Cas9 System. *Mol Ther Nucleic Acids* **7**, 11-19.
- 515 **Li, H. L., Fujimoto, N., Sasakawa, N., Shirai, S., Ohkame, T., Sakuma, T., Tanaka, M.,**  
516 **Amano, N., Watanabe, A., Sakurai, H. et al.** (2014). Precise Correction of the Dystrophin Gene  
517 in Duchenne Muscular Dystrophy Patient Induced Pluripotent Stem Cells by TALEN and CRISPR-  
518 Cas9. *Stem Cell Reports*.
- 519 **Long, C., Amoasii, L., Mireault, A. A., McAnally, J. R., Li, H., Sanchez-Ortiz, E.,**  
520 **Bhattacharyya, S., Shelton, J. M., Bassel-Duby, R. and Olson, E. N.** (2016). Postnatal genome  
521 editing partially restores dystrophin expression in a mouse model of muscular dystrophy.  
522 *Science* **351**, 400-3.
- 523 **Mamchaoui, K., Trollet, C., Bigot, A., Negroni, E., Chaouch, S., Wolff, A., Kandalla, P.**  
524 **K., Marie, S., Di Santo, J., St Guily, J. L. et al.** (2011). Immortalized pathological human  
525 myoblasts: towards a universal tool for the study of neuromuscular disorders. *Skelet Muscle* **1**,  
526 34.
- 527 **Morgoulis, D., Berenstein, P., Cazacu, S., Kazimirsky, G., Dori, A., Barnea, E. R. and**  
528 **Brodie, C.** (2019). sPIF promotes myoblast differentiation and utrophin expression while  
529 inhibiting fibrosis in Duchenne muscular dystrophy via the H19/miR-675/let-7 and miR-21  
530 pathways. *Cell Death Dis* **10**, 82.
- 531 **Muntoni, F., Frank, D., Sardone, V., Morgan, J., Schnell, F., Charleston, J., Desjardins,**  
532 **C., Phadke, R., Sewry, C., Popplewell, L. et al.** (2018). Golodirsen Induces Exon Skipping  
533 Leading to Sarcolemmal Dystrophin Expression in Duchenne Muscular Dystrophy Patients With  
534 Mutations Amenable to Exon 53 Skipping (S22.001). *Neurology* **90**.
- 535 **Muntoni, F., Torelli, S. and Ferlini, A.** (2003). Dystrophin and mutations: one gene,  
536 several proteins, multiple phenotypes. *Lancet Neurol* **2**, 731-40.
- 537 **Nelson, C. E., Hakim, C. H., Ousterout, D. G., Thakore, P. I., Moreb, E. A., Castellanos**  
538 **Rivera, R. M., Madhavan, S., Pan, X., Ran, F. A., Yan, W. X. et al.** (2016). In vivo genome  
539 editing improves muscle function in a mouse model of Duchenne muscular dystrophy. *Science*  
540 **351**, 403-7.
- 541 **Ousterout, D. G., Kabadi, A. M., Thakore, P. I., Majoros, W. H., Reddy, T. E. and**  
542 **Gersbach, C. A.** (2015). Multiplex CRISPR/Cas9-based genome editing for correction of  
543 dystrophin mutations that cause Duchenne muscular dystrophy. *Nat Commun* **6**, 6244.
- 544 **Pisani, C., Strimpakos, G., Gabanella, F., Di Certo, M. G., Onori, A., Severini, C.,**  
545 **Luvisetto, S., Farioli-Vecchioli, S., Carrozzo, I., Esposito, A. et al.** (2018). Utrophin up-  
546 regulation by artificial transcription factors induces muscle rescue and impacts the  
547 neuromuscular junction in mdx mice. *Biochim Biophys Acta*.

- 548 **Popplewell, L. J., Adkin, C., Arechavala-Gomez, V., Aartsma-Rus, A., de Winter, C. L.,**  
549 **Wilton, S. D., Morgan, J. E., Muntoni, F., Graham, I. R. and Dickson, G.** (2010). Comparative  
550 analysis of antisense oligonucleotide sequences targeting exon 53 of the human DMD gene:  
551 Implications for future clinical trials. *Neuromuscul Disord* **20**, 102-110.
- 552 **Ran, F. A., Hsu, P. D., Wright, J., Agarwala, V., Scott, D. A. and Zhang, F.** (2013).  
553 Genome engineering using the CRISPR-Cas9 system. *Nat Protoc* **8**, 2281-2308.
- 554 **Ricotti, V., Spinty, S., Roper, H., Hughes, I., Tejura, B., Robinson, N., Layton, G.,**  
555 **Davies, K., Muntoni, F. and Tinsley, J.** (2016). Safety, Tolerability, and Pharmacokinetics of  
556 SMT C1100, a 2-Arylbenzoxazole Utrophin Modulator, following Single- and Multiple-Dose  
557 Administration to Pediatric Patients with Duchenne Muscular Dystrophy. *PLoS ONE* **11**,  
558 e0152840.
- 559 **Roest, P. A., van der Tuijn, A. C., Ginjaar, H. B., Hoeben, R. C., Hoger-Vorst, F. B.,**  
560 **Bakker, E., den Dunnen, J. T. and van Ommen, G. J.** (1996). Application of in vitro Myo-  
561 differentiation of non-muscle cells to enhance gene expression and facilitate analysis of muscle  
562 proteins. *Neuromuscul Disord* **6**, 195-202.
- 563 **Ruiz-Del-Yerro, E., Garcia-Jimenez, I., Mamchaoui, K. and Arechavala-Gomez, V.**  
564 (2018). Myoblots: dystrophin quantification by in-cell western assay for a streamlined  
565 development of Duchenne muscular dystrophy (DMD) treatments. *Neuropathol Appl Neurobiol*  
566 **44**, 463-473.
- 567 **Tabebordbar, M., Zhu, K., Cheng, J. K. W., Chew, W. L., Widrick, J. J., Yan, W. X.,**  
568 **Maesner, C., Wu, E. Y., Xiao, R., Ran, F. A. et al.** (2016). In vivo gene editing in dystrophic  
569 mouse muscle and muscle stem cells. *Science* **351**, 407-411.
- 570 **Tinsley, J., Deconinck, N., Fisher, R., Kahn, D., Phelps, S., Gillis, J. M. and Davies, K.**  
571 (1998). Expression of full-length utrophin prevents muscular dystrophy in mdx mice. *Nat Med*  
572 **4**, 1441-4.
- 573 **Tinsley, J., Robinson, N. and Davies, K. E.** (2015). Safety, tolerability, and  
574 pharmacokinetics of SMT C1100, a 2-arylbenzoxazole utrophin modulator, following single-  
575 and multiple-dose administration to healthy male adult volunteers. *J Clin Pharmacol* **55**, 698-  
576 707.
- 577 **Tinsley, J. M., Blake, D. J., Roche, A., Fairbrother, U., Riss, J., Byth, B. C., Knight, A. E.,**  
578 **Kendrick-Jones, J., Suthers, G. K., Love, D. R. et al.** (1992). Primary structure of dystrophin-  
579 related protein. *Nature* **360**, 591-3.
- 580 **Tinsley, J. M., Potter, A. C., Phelps, S. R., Fisher, R., Trickett, J. I. and Davies, K. E.**  
581 (1996). Amelioration of the dystrophic phenotype of mdx mice using a truncated utrophin  
582 transgene. *Nature* **384**, 349-53.
- 583 **van Deutekom, J. C., Janson, A. A., Ginjaar, I. B., Frankhuizen, W. S., Aartsma-Rus, A.,**  
584 **Bremmer-Bout, M., den Dunnen, J. T., Koop, K., van der Kooij, A. J., Goemans, N. M. et al.**  
585 (2007). Local dystrophin restoration with antisense oligonucleotide PRO051. *N Engl J Med* **357**,  
586 2677-86.
- 587 **Wojtal, D., Kemaladewi, D. U., Malam, Z., Abdullah, S., Wong, T. W., Hyatt, E.,**  
588 **Baghestani, Z., Pereira, S., Stavropoulos, J., Mouly, V. et al.** (2015). Spell Checking Nature:  
589 Versatility of CRISPR/Cas9 for Developing Treatments for Inherited Disorders. *Am J Hum Genet.*
- 590 **Wright, A. V., Nunez, J. K. and Doudna, J. A.** (2016). Biology and Applications of  
591 CRISPR Systems: Harnessing Nature's Toolbox for Genome Engineering. *Cell* **164**, 29-44.
- 592 **Young, C. S., Hicks, M. R., Ermolova, N. V., Nakano, H., Jan, M., Younesi, S.,**  
593 **Karumbayaram, S., Kumagai-Cresse, C., Wang, D., Zack, J. A. et al.** (2016). A Single CRISPR-  
594 Cas9 Deletion Strategy that Targets the Majority of DMD Patients Restores Dystrophin  
595 Function in hiPSC-Derived Muscle Cells. *Cell Stem Cell* **18**, 533-40.

596

597

598 **Figure legends**

599 **Table 1. Off-target sites analyses.**

600 Top 6 off-target sequences of Ob1sgRNA2, Ob1sgRNA6, Ob2sgRNA22 and  
601 Ob2\_sgRNA26 identified with CRISPOR webtool, including the mismatches between  
602 sgRNAs, the off-target sequence, the chromosomes and loci targeted. All of them were  
603 analysed by PCR and Sanger sequencing, and no off-targets were detected.

604 **Figure 1. Editing approach and sgRNA design.**

605 (A and B). Schematic representation of our strategy for editing the *DMD* (A) and the  
606 *UTRN* loci (B). A pair of flanking sgRNAs are co-transfected in order to delete *DMD* exon  
607 52 (A) or the microRNA cluster contained in the 5'UTR of *UTRN* (B). (C and D). List of  
608 sgRNAs for editing the *DMD* (A) and the *UTRN* loci, showing sgRNAs sequences, PAM  
609 sequences and scores of all sgRNA tested. (E and F) Genomic location of the sgRNAs  
610 targeting the *DMD* (E) and *UTRN* loci (F).

611 **Figure 2. sgRNAs pairs test in 293 cells.**

612 (A and B). Representation of the different sgRNAs combinations tested for editing the  
613 *DMD* (A) and the *UTRN* loci (B). (C and D) Representative PCR analysis of HEK293 cells  
614 transfected with some of the sgRNAs combinations tested. Upper bands correspond to  
615 wild type or non-edited cells, while the lower bands correspond to the edited ones.  
616 Selected combinations are highlighted: Ob1sgRNA2+sgRNA6 (C);  
617 Ob2sgRNA22+sgRNA26 (D).

618 **Figure 3. Cloning and edition workflow, and efficiency diagram.**

619 (A) Scheme of the workflow followed to obtain the edited myoblast cell lines. 48 hours  
620 after plasmid transfection GFP positive myoblasts were single cell sorted using FACS.  
621 Clones were expanded until confluence for DNA extraction. (B) Efficiency of the  
622 different steps during the workflow process.

623

624

625 **Figure 4. Genotyping *DMD* and *UTRN* deletion breakpoints in edited myoblast clones.**

626 (A and B) PCR genotyping (A) and Sanger sequencing (B) of *DMD* edited clones (A). (C  
627 and D) PCR genotyping (C) and Sanger sequencing (D) of *UTRN* edited clones (A).  
628 Larger products in agarose gels (A and C) indicate non-edited clones, and shorter ones  
629 correspond with the expected deletion. (B and D) Sequences of the smaller bands  
630 confirmed the expected gene edition for objective 1: *DMD* $\Delta$ 52-Model and objective 2:  
631 *DMD*-*UTRN*-Model (B).

632 **Figure 5. Functional consequences of gene edition: dystrophin and utrophin**  
633 **expression.**

634 Dystrophin expression in control myoblasts compared to *DMD* $\Delta$ 52-Model cultures and  
635 *DMD* myoblasts studied by immunocytochemistry (A), western blotting (C) and  
636 myoblots (E) where n=24 wells per cell type were compared (\*\*\*\*p-value<0.0001).  
637 Utrophin expression in *DMD* myoblasts compared to *DMD*-*UTRN*-Model studied by  
638 immunocytochemistry (D), western blotting (E) and myoblots (F), where n=48 replicate  
639 wells were included per cell type. (\*\*\*\*p-value<0.0001) (P values were determined  
640 with Mann-Whitney U test).

641

642 **Figure 6. Evaluation of potential therapies in the generated cell culture models.**

643 A) *DMD* $\Delta$ 52-Model cell line was treated with an antisense to skip exon 51 and the  
644 effect was evaluated by RT-PCR and nested PCR analysis. Gel picture shows a pattern  
645 corresponding with the correct skipping, which was confirmed by Sanger sequencing.  
646 The same experiment evaluated by myoblot using n=20 wells per condition (B) showed  
647 the restoration of dystrophin expression in the treated cultures. (\*\*P values<0.05. P  
648 values were determined with Mann-Whitney U test).

649 C) The *DMD*-*UTRN*-Model was used as a positive control in an experiment in which  
650 unedited *DMD* cultures were treated with different ezutromid concentrations to up-  
651 regulate utrophin expression. Myoblot analysis using n=8 wells per condition of the  
652 treated cultures shows that ezutromid had no significant effect in *DMD* cultures while  
653 utrophin expression is significantly increased in *DMD*-*UTRN*-Model compared to

654 unedited DMD cultures. (\*\*P values<0.05. P values were determined with Mann-  
655 Whitney U test).

656

657 **Supplementary figure 1. PCR Analysis of Off Target Effects. Representative gel and**  
658 **sequence of PCR analysis performed for all targets.**

659 A) Agarose gel showing the amplification of the six predicted off-targets regions for  
660 sgRNA2 and the six for sgRNA6 (the combination used for our DMD edition model)  
661 amplified in control myoblasts and DMDΔ52-Model. B) All the amplicons were  
662 sequenced and no differences between control myoblasts and DMDΔ52-Model were  
663 found.

664 **Supplementary figure 2. MF20 differentiation marker depletion in edited cells.**

665 MF20 expression determined by myoblot in DMDΔ52-Model compared to control  
666 myoblasts (A) and in DMD-UTRN-Model compared to DMD myoblasts (B). Myoblot  
667 analysis was performed using n=12 (A) or n=18 (B) wells for MF20 staining. (\*\*P  
668 values<0.05; \*\*\*\* P values<0.0001 P values were determined with Mann-Whitney U  
669 test).

670

671 **Supplementary figure 3. Myoblasts transfection optimization and selection of positive**  
672 **cells by FACS.**

673 A) GFP expression 48h after transfection in control myoblasts using four different  
674 transfection reagents and following manufacturers conditions. B) Control myoblasts  
675 expressing GFP 48h post transfection with ViaFect® reagent and dot plot showing GFP  
676 positive cells (3,22%) selected using FACS.

677

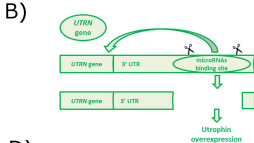
Off Target name	Guide sequence	Off target sequence	Mis	Chrom	Locus	PCR analysis	Sequencing
Ob1_2_Off1	GCTGAAGAACCCTGATACTAAGG (Ob1_sgRNA2)	GCTGGAGAACCCTGATACTGTGG	2	chr1	intergenic:RP4-781L3.1-RP4-706G24.1	No off target edition	Confirmed
Ob1_2_Off2		TCTGGAGAACCCTAATACTAAGG	3	chr8	intergenic:RP11-24P4.1-AC009695.1	No off target edition	Confirmed
Ob1_2_Off3		ACTGAAGAATCCAGAACTAGGG	4	chr7	intergenic:NOBOX-RP4-545C24.5	No off target edition	Confirmed
Ob1_2_Off4		GCTAGAGAAACCTGAACTAAGG	4	chr8	intergenic:RP11-536K17.1-EIF3H	No off target edition	Confirmed
Ob1_2_Off5		TCTGGAGAACCCTAATACTGTGG	4	chr3	intron:TMEM45A	No off target edition	Confirmed
Ob1_2_Off6		TCTGAAGAATCCTGATATTTTGG	4	chr2	intron:AC019100.3	No off target edition	Confirmed
Ob1_6_Off1	GACCAACAGCCAAGGATATGAGG (Obj1 sgRNA6)	CACCATCAGCCAAGAATATGCGG	3	chr11	intergenic:RP11-430H10.3-RP11-958J22.1	No off target edition	Confirmed
Ob1_6_Off2		TAAACAAGCCAAGACATGAGG	4	chr14	exon:RP11-1012A1.4/RDH11	No off target edition	Confirmed
Ob1_6_Off3		GTAAAAGAGCCAAGGATATGAGG	4	chr10	intron:RP11-556E13.1	No off target edition	Confirmed
Ob1_6_Off4		TACTAGCAGCCAAGGATATCTGG	4	chr2	intergenic:AC007377.1-SLC8A1	No off target edition	Confirmed
Ob1_6_Off5		GAGCGACAGCCAAGAATATTCGG	4	chr3	intron:CD96	No off target edition	Confirmed
Ob1_6_Off6		AATCAACAGCCAAGAATGTGGGG	4	chr5	intergenic:CTD-2201E9.4-SEMA5A	No off target edition	Confirmed
Ob2_22_Off1	GGTTCTTTAGCTGGGATCTGG (Obj 2 sgRNA22)	TGTTCTCTCTAACTGGGATCTGG	3	chr18	intergenic:RP11-411B10.6-RP11-411B10.5	No off target edition	Confirmed
Ob2_22_Off2		TGTTCTCTAGAGCTGGGATCTGG	3	chr21	intron:LCA5L	No off target edition	Confirmed
Ob2_22_Off3		TGTTCTCTCCTAACTGGGATCTGG	4	chr22	intron:PPP6R2	No off target edition	Confirmed

Ob2_22_Off4		GAATCCTTTTAGCTGGGATCAGG	4	chr19	intron:ZNF536	No off target edition	Confirmed
Ob2_22_Off5		GGTTCATCTTAGCTGGGATATGG	4	chr13	intron:FLT1	No off target edition	Confirmed
Ob2_22_Off6		TGTTCTCTCTAACTGGGGTCTGG	4	chr21	intergenic:PPP6R2P1-AP001347.6	No off target edition	Confirmed
Ob2_26_Off1	GTGCTTTCTGGGTATGACATGG (Obj2 sgRNA26)	AAGCTTTCCTGGATATGACAAGG	4	chr4	intron:RNF150	No off target edition	Confirmed
Ob2_26_Off2		GTGCTTACTGGGTAAGACGTGG	3	chr17	intergenic:RP11-212E8.1-RP11-642M2.1	No off target edition	Confirmed
Ob2_26_Off3		GAGTTAACTGGGTATGACAGGG	4	chr4	intron:RGS12	No off target edition	Confirmed
Ob2_26_Off4		GTGCTCTCATGAGAATGACAGGG	4	chr4	intergenic:GABRG1-RP11-320H14.1	No off target edition	Confirmed
Ob2_26_Off5		GAGCTTTCCTGGGAATGACAGGG	3	chr1	intergenic:FOXO6-RNA5SP45	No off target edition	Confirmed
Ob2_26_Off6		GTGCTTTATAGGATATAACATGG	4	chr6	intron:GSTA3	No off target edition	Confirmed

678

679 **Table 1. Potential off-target sites.**

680

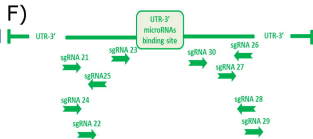
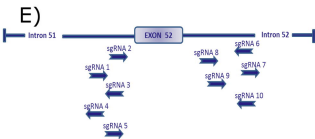


**C)**

CODE	SCORE	SEQUENCE	PAM
sgRNA1	79	CTGAAGAACCCTGATACTAA	GGG
sgRNA2	78	GCTGAAGAACCCTGATACTA	AGG
sgRNA3	69	AACAAATATCCCTTAGTATC	AGG
sgRNA4	65	ACAAATATCCCTTAGTATCA	GGG
sgRNA5	60	TAAGGGATATTTGTTCTTAC	AGG
sgRNA6	48	ATTTCTAAAAGTTTTGGC	TGG
sgRNA7	44	AAAAAAGATGTTACTGTATA	AGG
sgRNA8	44	AAAAAGATGTTACTGTATAA	GGG
gsRNA9	29	TTTACTTTGTATTATGTA	AGG
sgRNA10	24	TTTTATTCTAAAAGTGTTT	TGG

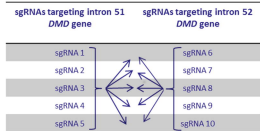
**D)**

CODE	SCORE	SEQUENCE	PAM
sgRNA21	71	AACTTTGGGTTCTCTTAGC	TGG
sgRNA22	66	GGTTCTCTTAGCTGGGATC	TGG
sgRNA23	63	TATTTAGAATAGGTTGGGT	GGG
sgRNA24	62	ACTTTGGGTTCTCTTAGCT	GGG
sgRNA25	62	TCTAACTTTAAGCCTCCTTC	TGG
sgRNA26	76	GTGCTTCTTGGGTATGACA	TGG
sgRNA27	68	CAAAGTCTAGAGCTTTTATC	AGG
sgRNA28	66	CAACTTGGAGTTGAGAGCTC	AGG
sgRNA29	64	TCAACTCCAAGTTGTAGATT	TGG
sgRNA30	63	TCCATCTTCATCCATTGCAT	TGG

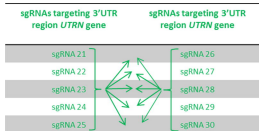




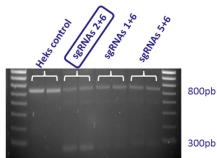
A)



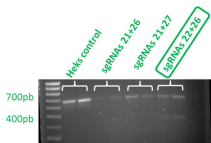
B)



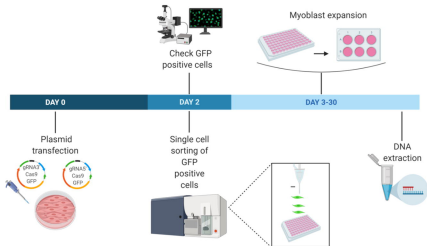
C)



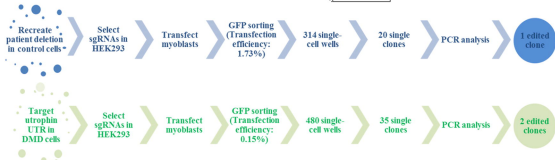
D)



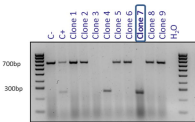
A)



B)



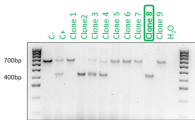
A)

Clone 7 = DMD $\Delta$ 52-Model

B)

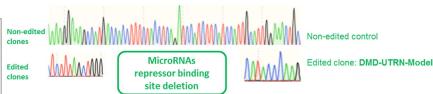


C)

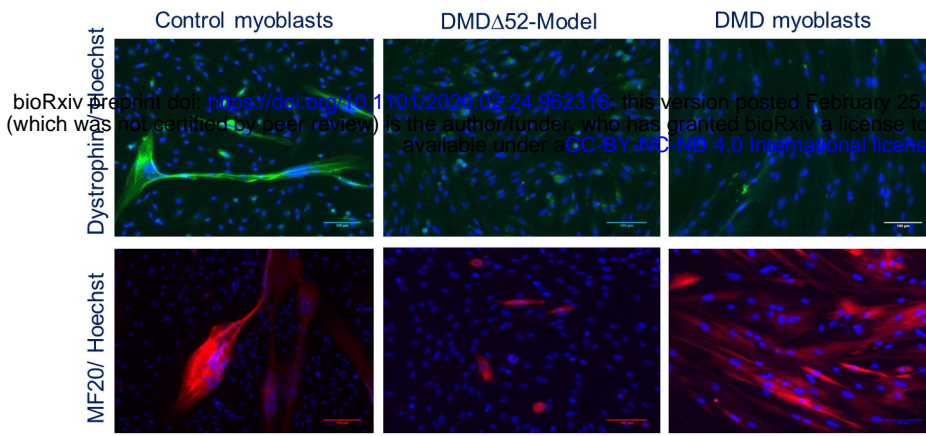


Clone 8 = DMD-UTRN -Model

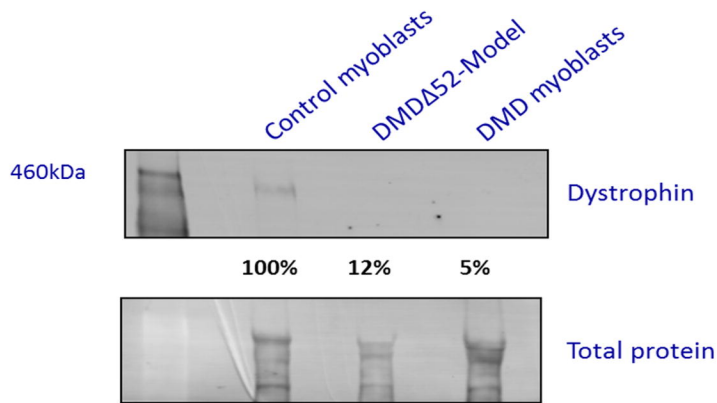
D)



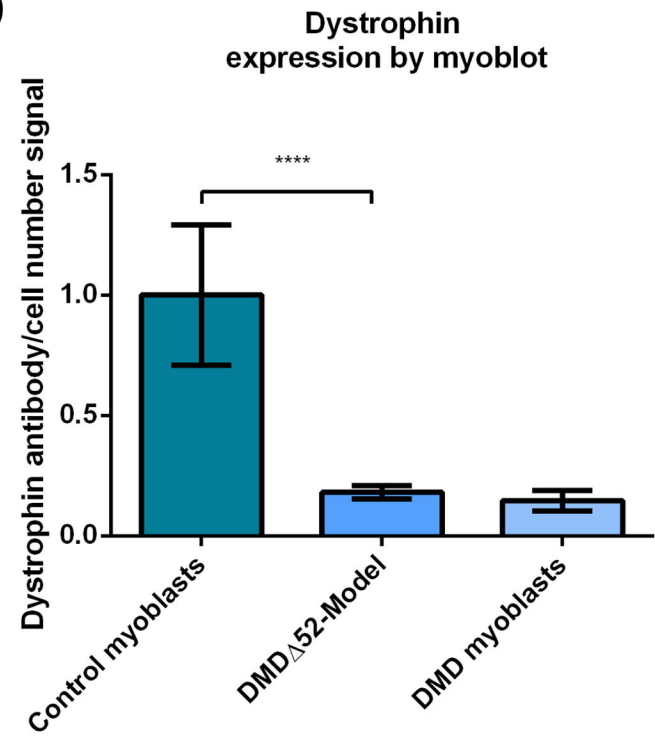
A)



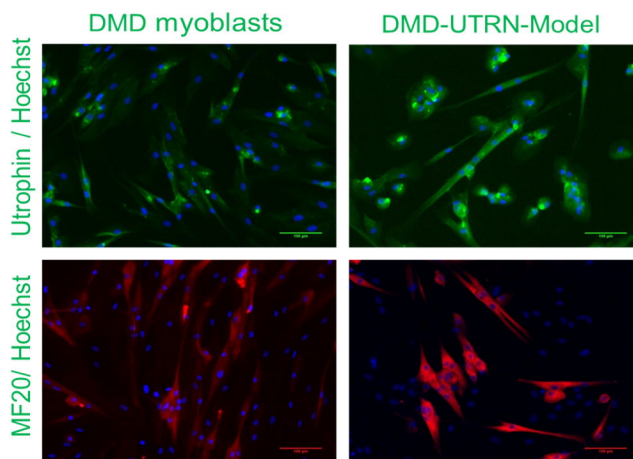
B)



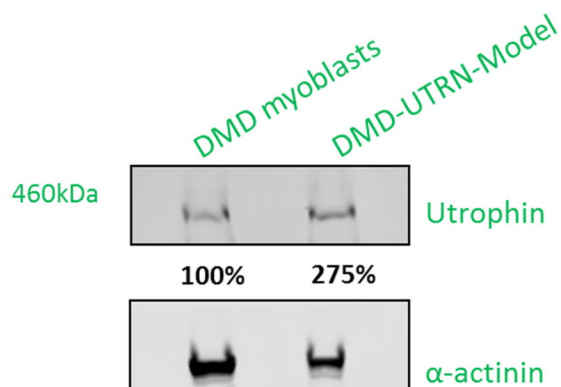
C)



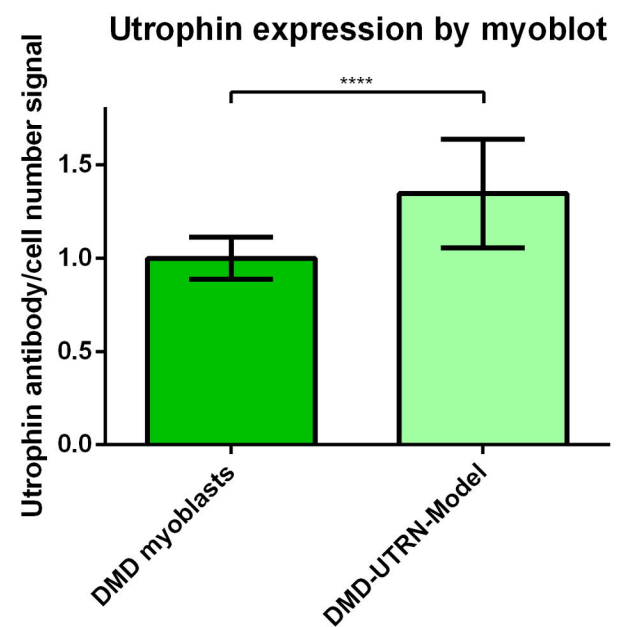
D)



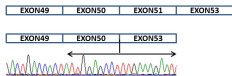
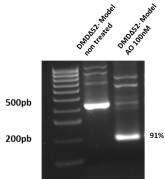
E)



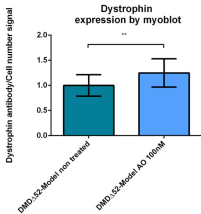
F)



A)



B)



C)

